Applied Catalysis B: Environmental 142–143 (2013) 222–233

Contents lists available at SciVerse ScienceDirect

Applied Catalysis B: Environmental

journal homepage: www.elsevier.com/locate/apcatb

The effect of TiO_2 doping on catalytic performances of Ru/CeO_2 catalysts during catalytic combustion of chlorobenzene

Qiguang Dai*, Shuxing Bai, Jianwei Wang, Meng Li, Xingyi Wang*, Guanzhong Lu

Lab for Advanced Materials, Research Institute of Industrial Catalysis, East China University of Science and Technology, Shanghai 200237, PR China

ARTICLE INFO

Article history:
Received 18 January 2013
Received in revised form 3 April 2013
Accepted 13 May 2013
Available online 23 May 2013

Keywords:
Chlorobenzene
Catalytic combustion
Ruthenium
Titanium
Ceria

ABSTRACT

The lower temperature catalytic combustion of chlorinated hydrocarbons (CHCs), including chlorobenzene (CB), 1,2-dichloroethane (DCE) and trichloroethylene (TCE), over RuO_2 supported on Ti-doped CeO_2 catalysts ($Ru/Ti–CeO_2$) was investigated, and the effects of preparation methods, Ti content, Ru content, inlet CB concentration and space velocity, oxygen concentration and water were studied detailedly. Moreover, the doping of other different metals (Mn, Co, Sn and Mg) and the supporting of different precious metals (Pt, Pd, Rh, Au and Ag) also were briefly explored. The results show that the doping of Ti can improve obviously the catalytic activity and stability of CeO_2 based catalysts. The better catalytic activity of $Ru/Ti–CeO_2$ is ascribed to the expose of more oxygen vacancies and high energy lattice plane CeO_2 (1 1 0) and (1 0 0), and the Cl dissociatively adsorbed at active sites of CeO_2 can be oxidized into Cl_2 catalyzed by RuO_2 supported $Ti–CeO_2$ at lower temperature (such as 200 °C) which be responsible to the excellent stability of $Ru/Ti–CeO_2$ catalysts.

1. Introduction

The emission of dioxin, namely polychlorinated dibenzodioxins and polychlorinated dibenzofurans (PCDD/Fs), from the flue gas of municipal waste incinerations, metallurgical industry, the chlorine bleaching process in pulp and paper industry and cogeneration units fed with biomass are well-known to be responsible for carcinogenic, hormonal problems and the depletion of the ozone layer in the stratosphere [1,2]. Therefore, stringent environmental regulations are in place in many countries to limit PCDD/Fs emission [3]. The reduction/elimination of PCDD/Fs has thus been received much attention and extensive effort has been made toward the destruction of PCDD/Fs. As far as we know, the catalytic total oxidation or combustion of PCDD/Fs to CO_2, HCl, and H_2O over proper catalysts has been confirmed to be one of the best methods, and the major advantage is that the reaction can be efficiently performed at relatively low temperatures, and very dilute pollutants can be treated efficiently. Normally, considering PCDD/Fs' high toxicity and delicate manipulation in laboratories, model compounds have been used to evaluate the activity of the catalysts in the majority of these studies. Chlorobenzene (CB) and 1,2-dichlorobenzene (*o*-DCB) have been most frequently used [3], because of their structural similarity to PCDDs.

For the catalytic combustion of PCDD/Fs, the research and development of novel catalysts with high performances at low temperature is still crucial. In the last two years, of all the reported studies of the catalysts for catalytic combustion of CB and *o*-DCB, most are focused on two types of catalysts based on noble metals [4–6] and transition metal oxides (such as V_2O_5 [7–9], CuO [10,11], MnO_x [12,13] and Cr_2O_3 [14]). In general, noble metals based catalysts show the highest activity. However, they undergo deactivation due to chlorine poisoning and polychlorinated compounds formation. Alternatively, much effort has been devoted to the transition metal oxides catalysts, especially the transition metals doped or supported TiO_2 catalysts, mainly including V [7–9,15–18], Zr [19,20], Co [21], Fe [22] and Mn [23,24] doped or supported TiO_2 catalysts. In practical, V_2O_5/TiO_2 based catalysts are commercially employed and have also been found to be most active and stable for the oxidation of PCDD/Fs. Among all of the above catalysts, the main role of TiO_2 includes: (1) improving the dispersion of transition metals on the supports [15,22–24]; (2) improving the redox performance of catalysts [23] and enhancing the oxygen mobility by the creation of oxygen vacancies due to a better reducibility of the TiO_2 support (Ti^{4+} into Ti^{3+}) [19]; (3) exhibiting a high resistance against HCl and being a stable support [15,25]; and (4) supplying the Lewis acid sites for the adsorption and dissociation of chlorobenzene molecules [16,22]. Additionally, the crystal phase of TiO_2 also is important and the existence of a small amount of rutile phase of TiO_2 may increase the catalytic activity [23].

In previous work [12,26,27], we found that CeO_2 based catalysts showed a higher catalytic activity for the catalytic combustion of

* Corresponding authors. Tel.: +86 21 64253183; fax: +86 21 64253372.
E-mail addresses: daiqg@ecust.edu.cn, vistadai@163.com (Q. Dai), gzhlu@ecust.edu.cn (X. Wang), gzhlu@ecust.edu.cn (G. Lu).

0926-3373/$ – see front matter © 2013 Elsevier B.V. All rights reserved.
http://dx.doi.org/10.1016/j.apcatb.2013.05.026

chlorobenzene, but a better stability only was achieved at a higher temperature (that more higher than the complete combustion temperature). Our recent studies [28,29] show that the doping of Ru into CeO_2 can evidently improve the stability of CeO_2 based catalysts at lower temperature and the deactivation is not observed within 82 h at 275 °C. The better stability of the Ru–CeO_2 catalysts can be ascribed to the dissociatively adsorbed Cl species on active sites can be removed rapidly in form of Cl_2 via the Deacon process catalyzed by RuO_2 component. However, the temperature to obtain stable activity is still too high, which results in the formation of a large amount of dichlorobenzene by-products is unavoidable. Thus, achieving a lower temperature without deactivation, namely enhancing the activity of catalysts for the oxidation of the adsorbed Cl species into Cl_2, still is a key problem to be solved for the Ru–CeO_2 catalysts.

Recently, the numerous literatures reported that RuO_2 catalysts supported on rutile-type carriers (TiO_2 [30,31], SnO_2 [32,33]) exhibit high activity and a long lifetime in the oxidation of HCl into Cl_2 (Deacon Reaction), practically RuO_2/TiO_2-rutile was commercialized by Sumitomo in 2002 and RuO_2/SnO_2-cassiterite also was successfully piloted by Bayer [34]. The studies have shown that the choice of the carrier for ruthenium is crucial to obtain a superior Deacon catalyst, for example, RuO_2/TiO_2-rutile is at least 10 times more active than RuO_2 on traditional SiO_2 and Al_2O_3 supports, which can be ascribed to the following two reasons [34]: (1) RuO_2 possesses similar lattice parameters with a rutile-type structural TiO_2 or SnO_2; (2) RuO_2 on TiO_2-rutile or SnO_2-cassiterite features a thin film coating the carrier, which both are favor to maximize metal dispersion and improve structural stability.

Therefore, it can be speculated that the doping of Ti or Sn into Ru–CeO_2 catalyst would further improve the catalytic performance of CeO_2 based catalysts for the catalytic combustion of chlorinated hydrocarbons, especially the stability of catalysts at lower temperature. In the present work, the effect of TiO_2 doping on catalytic performances of Ru/CeO_2 catalysts during catalytic combustion of chlorobenzene was investigated, including the preparing methods, the content of TiO_2 and RuO_2, space velocity, water vapor, and the concentration of chlorobenzene and oxygen. In addition, the effect of the doping of other metal oxides (such as Sn, Co, Mg and Mn) and the loading of several noble metals (such as Au, Rh, Ag, Pt and Pd) on the catalytic combustion of various chlorinated hydrocarbons (such as 1,2-dichloroethane (DCE), trichloroethylene (TCE) and CB) was also examined.

2. Experimental

2.1. Catalysts preparation

2.1.1. Preparation of Ti doped CeO_2

2.1.1.1. Co-precipitation method. The typical synthesis procedure of co-precipitation method, $Ce(NH_3)_2(NO_3)_6$ (10 g) was dissolved in the deionized water (25 mL), and stoichiometric amounts of tetrabutyl titanate ($Ti(OC_4H_9)_4$, 0.21 mL) or titanium tetrachloride ($TiCl_4$, 0.18 g) was added into the $Ce(NH_3)_2(NO_3)_6$ solution under vigorously stirring. The solution was stirred at room temperature for 0.5 h, and then a 15 wt% NaOH solution (50 mL) was added dropwise into the above solution. After the solution was stirred at room temperature for 2 h, and the suspension was aged at room temperature for 48 h. Subsequently, the precipitates were washed with distilled water and ethanol, dried at 80 °C overnight, followed by calcinations at 450 °C for 3 h in air. The sample prepared by tetrabutyl titanate as the precursor was marked as Ti–CeO_2-CP(TBT), and titanium tetrachloride as the precursor was labeled as Ti–CeO_2-CP($TiCl_4$).

2.1.1.2. Sol–gel method. The typical synthesis procedure of water phase sol–gel method, a solution of tetrabutyl titanate ($Ti(OC_4H_9)_4$, 0.21 mL) and nitric acid (2 drops) in ethanol (5 mL) with moderate agitation was added to a mixture of ammonium ceric nitrate ($Ce(NH_3)_2(NO_3)_6$, 10 g) or cerium (III) nitrate hexahydrate ($Ce(NO_3)_3{\cdot}6H_2O$, 7.92 g) and citric acid (1.15 g) in deionized water (75 mL), and was stirred at 80 °C until the formation of gel. The obtained gel was aged at 110 °C for 10 h, followed by calcinations at 450 °C for 3 h in air. The resulting catalysts were designated Ti–CeO_2-SGIV and Ti–CeO_2-SGIII, respectively.

2.1.1.3. Incipient wetness impregnation method. The detail procedures of incipient wetness impregnation method was as follows: 1.0 g of CeO_2 prepared by the same method with Section 2.1.1 was added to a solution of tetrabutyl titanate ($Ti(OC_4H_9)_4$, 0.21 mL) and deionized water (1 mL). After impregnation and drying overnight in air at 80 °C, the resulting powder was calcined in air at 450 °C for 3 h. The resulting catalysts were designated Ti–CeO_2-IM.

2.1.2. Preparation of other metals doped CeO_2

The other metals (such Sn, Mn, Co, Mg) doped CeO_2 composite oxide catalysts were prepared by the same co-precipitation method with Section 2.1.1. The used precursor was tin (II) chloride dehydrate ($SnCl_2{\cdot}2H_2O$, 0.21 g), 50% manganous nitrate ($Mn(NO_3)_2$, 0.34 mL), cobaltous nitrate hexahydrate ($Co(NO_3)_2{\cdot}6H_2O$, 0.23 g) and magnesium nitrate hexahydrate ($Mg(NO_3)_2{\cdot}6H_2O$, 0.25 g), respectively.

2.1.3. Preparation of supported precious metals catalysts

Supported precious metals catalysts were prepared by the incipient wetness impregnation and deposition precipitation method using various precious metals precursor. A typical incipient wetness impregnation procedure was as follows: the Ti–CeO_2 support was impregnated with an aqueous solution containing an appropriate amount of ruthenium (III) chloride, or chloroauric acid ($HAuCl_4$), silver nitrate ($AgNO_3$), rhodium (III) chloride ($RhCl_3$), chloroplatinic acid (H_2PtCl_6), palladium chloride ($PdCl_2$), and then dried at 80 °C for 12 h and calcined in air at 450 °C for 3 h. Briefly, for the deposition precipitation method the Ti–CeO_2 support was suspended in an aqueous solution containing various precious metals precursor and continuously stirred at 50 °C. Afterwards, NaOH (0.1 M) solutions were added to the above suspension. Finally, the solid was filtered, washed with deionized water and dried at 80 °C for 12 h and calcined in air at 450 °C for 3 h.

2.2. Catalysts characterization

The powder X-ray diffraction (XRD) patterns of samples were recorded on a Rigaku D/Max-rC powder diffractometer using Cu Kα radiation (40 kV and 100 mA). The nitrogen adsorption and desorption isotherms were measured at 77 K on an ASAP 2400 system in static measurement mode. Ruthenium and Ti content was determined by X-ray fluorescence (XRF) using a Shimadzu (XRF-1800) wavelength dispersive X-ray fluorescence spectrometer. The XPS measurements were made on a VG ESCALAB MK II spectrometer by using Mg Kα (1253.6 eV) radiation as the excitation source. H_2-temperature programmed reduction (H_2-TPR) of samples (200 mg) placed at the bottom of the U-shaped quartz tube was investigated, and the extent of reduction was quantitatively calculated according to the TPR peak areas and the result was calibrated on the basis of the hydrogen consumption from the reduction of CuO to Cu. High-resolution transmission electron microscopic (HRTEM) images were taken on a JEM-2100F field emission transmission electron microscope that operated at 200 kV.

2.3. Catalytic activity measurements

Catalytic combustion reactions were carried out in a continuous flow micro-reactor constituted of a U-shaped quartz tube of 3 mm of inner diameter at atmospheric pressure. 200 mg catalyst was placed at the bottom of the U-shaped micro-reactor. The feed flow through the reactor was set at 40 cm^3 min^{-1} and the gas hourly space velocity (GHSV) was maintained at 15,000 h^{-1}. Feed stream to the reactor was prepared by delivering liquid CB with a syringe pump into dry air and the injection point was electrically heated to ensure complete evaporation of the liquid reaction feeds. The concentration of CB in the reaction feeds was set at 550 ppm. The water vapor fed into the system was made by bubbling air into water in a temperature-controlled saturation system (25 °C). In order to minimize the possible adsorption of the CB on the inner surface of piping, the piping was heated (T = 120 °C) by a heater band. The temperature of the reactor was measured with a thermocouple located just at the bottom of the micro-reactor and the effluent gases were analyzed by an on-line gas chromatograph equipped with a flame ionization detector (FID). Catalytic activity was measured over the range 100–400 °C and conversion data were calculated by the difference between inlet and outlet concentrations. Conversion measurements and product profiles were taken after maintained for 5 min at each test temperature. Additionally, mass spectrum was used for the determination of the main intermediates and by-products.

The temperature-programmed surface reaction (TPSR) measurement was carried out under the catalytic activity tests condition. First, the air flow containing 1500 ppm CB flowed continuously the catalysts at 100 °C. After the adsorption–desorption reached an equilibrium, the catalysts were heated from 100 °C to a specified temperature at 10 °C min^{-1}. The reactant and the products (such as CB (m/z = 112), CO_2 (44), CO (28), Cl_2 (70), HCl (36), dichlorobenzene (146), and B (78)) were analyzed on-line over a mass spectrometer apparatus (HIDEN QIC-20).

3. Results and discussion

3.1. Effect of preparation methods

The conversion of chlorobenzene over Ti–CeO_2 catalysts prepared by different methods (Fig. 1A) and the corresponding supported 1%Ru/Ti–CeO_2 catalysts prepared by the incipient wetness impregnation method (Fig. 1B) are shown in Fig. 1. Among all the Ti–CeO_2 catalysts, the Ti–CeO_2-IM showed the worst activity and the conversion of chlorobenzene was under 30% even at 300 °C, which possibly results from the cover or block of TiO_2 on CeO_2 active sites. Other Ti–CeO_2 catalysts all presented a better activity but were slightly less than pure CeO_2 catalyst (see Fig. 2A), and even the 80% conversion of chlorobenzene over Ti–CeO_2-CP(TBT) and Ti–CeO_2-SGIII catalysts can be achieved before 200 °C. However, the evident deactivation was observed on all the Ti–CeO_2 catalysts and the introduction of individual Ti cannot improve the stability of CeO_2 based catalysts. From Fig. 1B, it can be found that the catalytic activity of 1%Ru/Ti–CeO_2 catalysts except the 1%Ru/Ti–CeO_2-IM decreased obviously in the lower temperature ranges, compared with the corresponding Ti–CeO_2 catalysts. The decrease of activity still may be ascribed to the occupation of active sites by Ru species dispersed on the surface of CeO_2. However, the stability of Ti–CeO_2 catalysts is improved significantly and the further discussions would be given in the later sections. Additionally, it can be found that the 1%Ru/Ti–CeO_2-CP(TBT) catalyst possesses the best activity and also more higher than that of 1%Ru/CeO_2 catalyst [28]. Therefore, the co-precipitation method with tetrabutyl titanate as the precursor is used for the following tests unless stated otherwise.

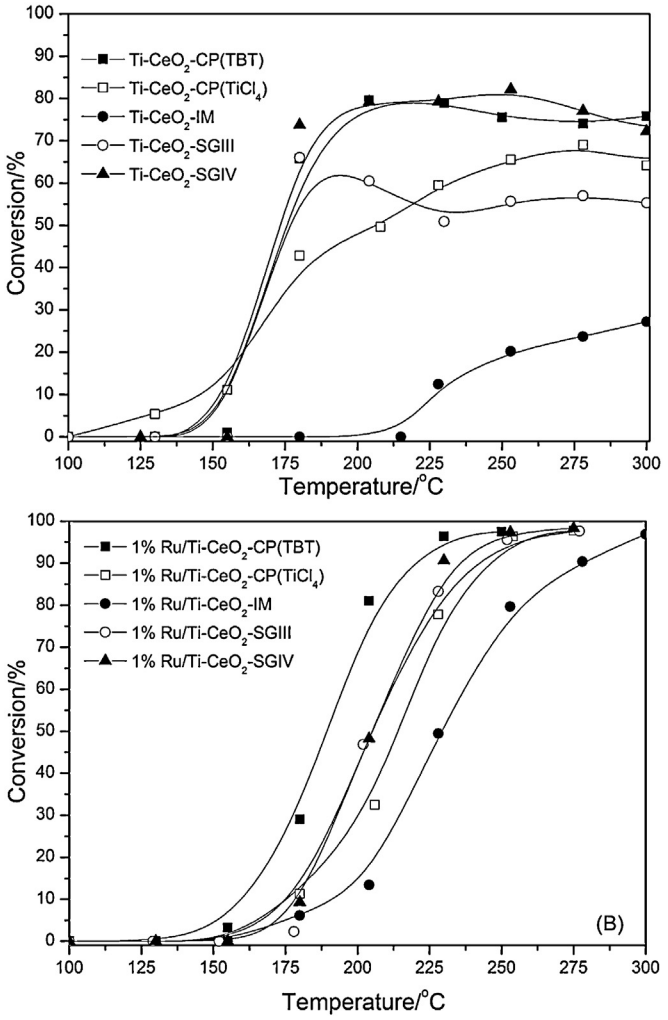

Fig. 1. Conversion of chlorobenzene over Ti–CeO_2 prepared by different methods and the corresponding 1%Ru supported Ti–CeO_2 catalysts. CB concentration: 550 ppm; GHSV: 15,000 h^{-1}; catalyst amount: 200 mg.

3.2. Effect of Ti content

The influence of the Ti content doped into CeO_2 on the catalytic combustion of chlorobenzene was studied, and the results are shown in Fig. 2. As shown in Fig. 2A, two different series of activity curves are observed according to the content of Ti doped CeO_2. For the Ti–CeO_2 catalysts containing Ti content from 1% to 25%, the difference between activities is almost negligible. However, after the content of Ti is more than 25%, the catalytic activities obviously decrease with the increase of Ti and is much lower than that of CeO_2, even the conversion is lower than 10% at 400 °C on the pure TiO_2 catalyst. This result also indicates that TiO_2 is inactive for the catalytic combustion of chlorobenzene. Fig. 2B gives the conversion curves of chlorobenzene on 1%RuO_2 supported Ti–CeO_2 with different Ti content catalysts. Visually, the deactivation during activity tests is not observed, and similar with the results in Fig. 1B. The activities of 1%RuO_2/Ti–CeO_2 catalysts increase with the increase of Ti doping content, and 5% and 10% Ti doping catalysts show the highest and similar activities. However, after the doping content of Ti is more than 10%, the activities of 1%RuO_2/Ti–CeO_2 catalysts are significantly decreased, even the catalysts containing more 50% Ti only exhibit almost negligible activities and the conversion are less than 20% at 400 °C. Unexpectedly, it can be found that the activities of 1%RuO_2/Ti–CeO_2 catalysts containing more 50% Ti are lower than the 1%RuO_2/SBA-15 catalyst [28], the possible

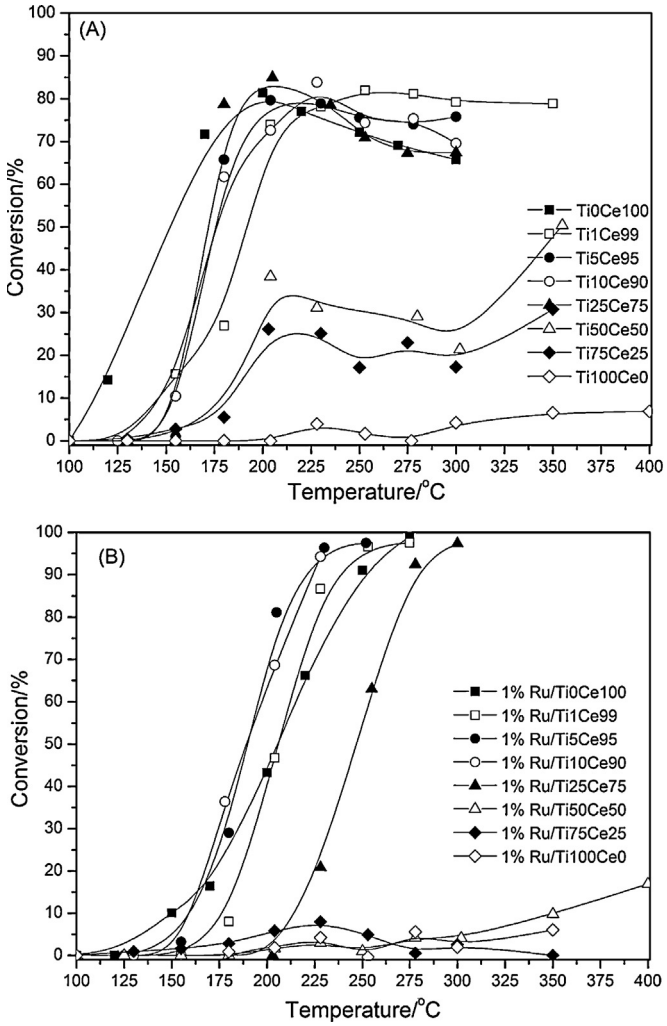

Fig. 2. Conversion of chlorobenzene over Ti–CeO_2 and 1%Ru/Ti–CeO_2 catalysts doped different amounts of Ti. CB concentration: 550 ppm; GHSV: 15,000 h^{-1}; catalyst amount: 200 mg.

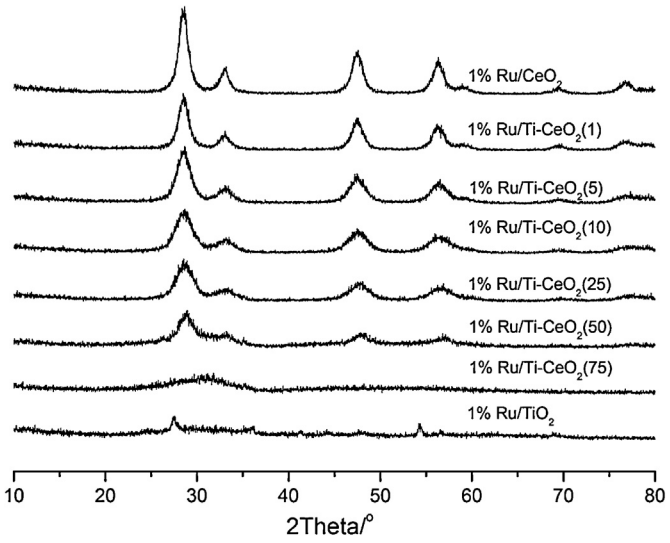

Fig. 3. XRD patterns of 1%Ru/Ti–CeO_2 catalysts doped different amounts of Ti.

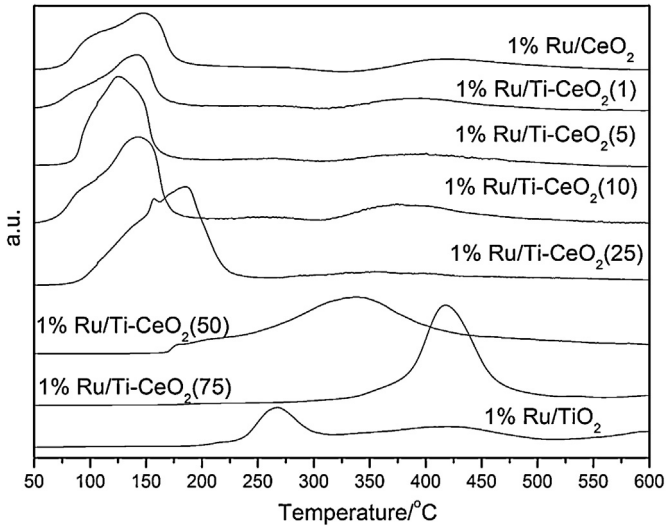

Fig. 4. H_2-TPR profiles of 1%Ru/Ti–CeO_2 catalysts with different Ti contents.

reasons result from the activity of Ru supported the non-ceria supports (such as TiO_2 and SiO_2) catalyst is mainly ascribed to the particles size and dispersion of RuO_2 depended on the surface area of supports. Interestingly, the color of catalysts is changed remarkably from dark brown to light brown (Ti content increases from 1% to 10%), grayish green to green (Ti content increases from 25% to 75%) and eventually appears gray (1%Ru/TiO_2), the photos are shown in Fig. 1S, which corresponds to the changes of the activity.

Fig. 3 shows the XRD patterns of 1%Ru/Ti–CeO_2 samples doped different amounts of Ti. No crystalline phase ascribed to ruthenium oxide can be found in the all 1%Ru/Ti–CeO_2 samples, indicating that either RuO_2 is present as a noncrystalline phase or the particle size is smaller than 3 nm and finely dispersed on the Ti–CeO_2 supports. The 1%Ru/Ti–CeO_2 samples with Ti content between 0% and 75% exhibit only the characteristic peaks of the cubic fluorite structure of CeO_2 at 28.7°, 33.1°, 47.4°, 56.3°, 69.7° and 76.9°, and the crystallite sizes and lattice parameters of CeO_2 decrease with the doping of Ti (Table 1). However, the XRD patterns of 1%Ru/Ti–CeO_2(75) sample only shows a broad peak between 25° and 35°, which indicates that the sample is an amorphous structure. For the 1%Ru/TiO_2 sample, it is difficult to clearly determine the assignment of peaks at about 28°, 35° and 55° due to RuO_2 and rutile TiO_2 possessing similar XRD patterns (see Fig. 2S). Fig. 3S gives the XRD pattern of pure TiO_2, it can be found that the pure TiO_2 prepared by precipitation method also is amorphous and same with the 1%Ru/Ti–CeO_2(75) sample. Therefore, it can confirm that the peaks is ascribed to the RuO_2 phase in the 1%Ru/TiO_2 sample, which also indicates that the crystallite size of RuO_2 in the 1%Ru/TiO_2 sample is larger compared with 1%Ru/SBA-15 [28]. Thus, 1%Ru/TiO_2 catalyst presents a very poor activity for the CB catalytic combustion. Additionally, the amorphous structure of TiO_2 in the 1%Ru/Ti–CeO_2 catalysts with a higher content of Ti may be another reason for its low activity, and our ongoing works also show that crystalline Ti–CeO_2, Ru/Ti–CeO_2 and Ru/TiO_2 catalysts present a better activity for the catalytic combustion of chlorobenzene and 1,2-dichlorobenzene.

TPR profiles of 1%Ru/Ti–CeO_2 catalysts with different Ti contents are shown in Fig. 4, and the amounts of hydrogen consumption of all catalysts during TPR measurement are summarized in Table 1. Two series of reduction peaks, low-temperature peak (LT, 75–300 °C) and high-temperature peak (HT, 325–500 °C), are observed for the all samples except for 1%Ru/Ti–CeO_2(50) and 1%Ru/Ti–CeO_2(75) catalysts. The former is attributed to the reduction of RuO_2 and the latter is corresponded to surface capping oxygen species of CeO_2 and/or TiO_2 [35]. The position of the low-temperature peak shifts to lower temperatures with the increase of TiO_2 content from 0% to 5%, and then quickly shifts to higher temperatures. The results

Table 1
Surface and structural properties of Ru based and pure CeO_2 catalysts.

Catalyst	RuO_2 content[a]	TiO_2 content[a]	S_{BET} ($m^2\ g^{-1}$)[b]	Crystallite size (nm)[c]	Lattice parameters (nm)[d]	H_2 consumption (μmol/g cat)[e]	
						LT	HT
CeO_2 [28]	0	0	100.8	7.4	0.5413	0	410
1%Ru/CeO_2	1.14	0	82.4	6.8	0.5387	740	84
1%Ru/Ti–CeO_2(1)	1.08	0.59	82.1	6.2	0.5413	513	189
1%Ru/Ti–CeO_2(5)	1.15	2.0	113.2	4.5	0.5391	806	77
1%Ru/Ti–CeO_2(10)	1.04	4.9	118.7	3.8	0.5416	879	230
1%Ru/Ti–CeO_2(25)	1.16	13.0	118.3	3.7	0.5409	1166	75
1%Ru/Ti–CeO_2(50)	1.05	25.3	87.5	3.7	0.5333	1019	
1%Ru/Ti–CeO_2(75)	1.03	51.3	89.0	–	–	938	
1%Ru/TiO_2	1.10	98.0	60.8	–	–	199	153

[a] RuO_2 and TiO_2 content (wt.%) measured by XRF.
[b] BET surface area.
[c] The crystallite sizes of the CeO_2(1 1 1) were calculated from X-ray diffraction line broadening using the Scherrer equation.
[d] Lattice parameters calculated from XRD results.
[e] Calculated from TPR results.

are consistent with the activities of catalysts. Moreover, a shoulder peak can be observed in the lower temperature ranges for the 1%Ru/Ti–CeO_2 catalysts with Ti content lower than 50%, which could be tentatively assigned to the reduction of the finely dispersed RuO_2 species, while the main peak could be ascribed to the reduction of both ruthenium oxide species with strong interaction with the support [36]. However, for 1%Ru/Ti–CeO_2(50) and 1%Ru/Ti–CeO_2(75) catalysts, the H_2-TPR only gives one reduction peak between 200 and 500 °C, which probably comes from the strong interaction of RuO_2 species with the Ti–CeO_2 support with higher Ti content and the changes of natures of supports (the doping of Ce into TiO_2). According to Table 1, the hydrogen consumption for the LT peak, ascribed to the reduction of RuO_2 species, increases with increasing TiO_2 content except for the 1%Ru/Ti–CeO_2(1) catalyst, and reaches a maximum at 25% and represents around ten times the hydrogen needed for the total reduction of the ruthenium oxide. This fact indicates that some part of the CeO_2 in the vicinity of the Ru crystallites are reduced in similar way that for Pt–CeO_2 materials [37].

Due to 1%Ru/Ti–CeO_2(5) shows the best catalytic activity and redox ability, and it is TEM and HRTEM are investigated. The TEM images of 1%Ru/CeO_2 and 1%Ru/Ti–CeO_2(5) (see Figs. 5S and 6S) samples demonstrate that the both samples have irregular shape and about 6.6 nm and 4.8 nm mean diameter, respectively. This value is in good agreement with the average mean diameter which arise from the application of the Scherrer equation on the XRD data (see Table 1). Additionally, the typical HRTEM images of the samples are shown in Fig. 5, which exhibit clear lattice images of CeO_2, but undistinguishable crystalline RuO_2 particles on supports, which probably attributes to the smaller particles size of RuO_2 highly dispersed on CeO_2 (as the detection limit of the HRTEM technique is around 1 nm) or the formation of Ru–CeO_2 solid solution. According to FFT analysis, it can be found that three kinds of lattice fringe directions attributed to (1 1 1), (2 0 0) and (2 2 0) of CeO_2 were observed for the both samples, which have a respective interplanar spacing of 0.31, 0.27 and 0.19 nm. However, the lattice fringes of RuO_2 and TiO_2 are very difficult to be found likely due to the similar crystal structure and interplanar spacing with CeO_2. Moreover, the XRD results showed the TiO_2 is amorphous after the higher content of Ti was doped into CeO_2 (such as 75% and 100%), thus it can be inferred that the TiO_2 phase may be existed in the 1%Ru/Ti–CeO_2(5) sample in form of amorphous structure and there will be no lattice fringes of TiO_2 can be observed on the HRTEM images. Similarly, RuO_2 also might be present as a noncrystalline phase. In particular, in can be found that the ratio of the exposed high energy lattice plane (2 2 0) and (2 0 0) and the low energy lattice plane

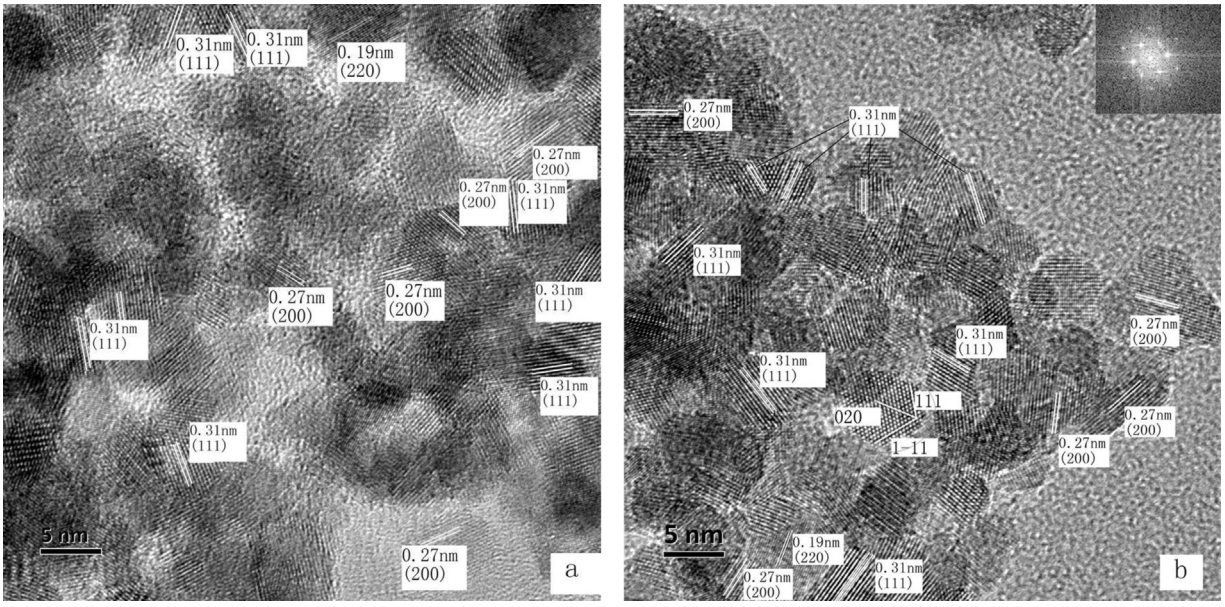

Fig. 5. HRTEM images of 1%Ru/CeO_2 (A) and 1%Ru/Ti–CeO_2 (B) samples.

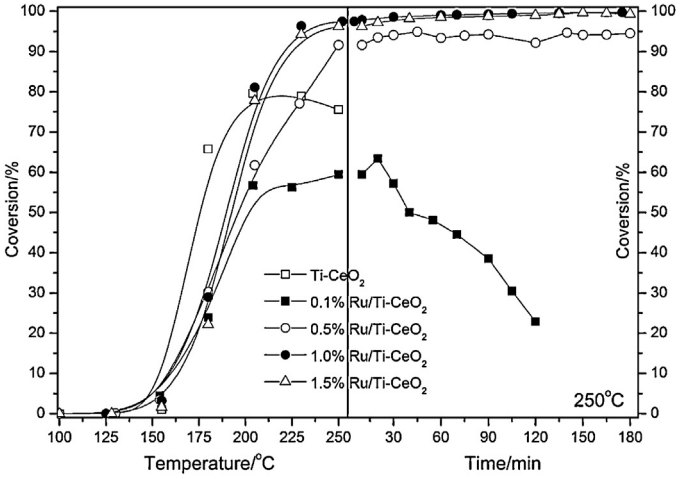

Fig. 6. The light-off curves of CB catalytic combustion over Ru/Ti–CeO_2 catalysts supported different Ru contents. CB concentration: 550 ppm; GHSV: 15,000 h^{-1}; catalyst amount: 200 mg.

(1 1 1) in the both samples is more than 50%, and 1%Ru/Ti–CeO_2(5) sample exposes more (2 2 0) and (2 0 0) lattice plane. Our previous work suggested that the CeO_2 nanorod exposed (1 1 0) and (1 0 0) crystal planes showed the highest activity for the catalytic combustion of 1,2-dichloroethane [38]. Therefore, we consider that the higher activity of 1%Ru/Ti–CeO_2(5) sample benefits from the more exposed high energy lattice plane. Interestingly, a small amount of CeO_2 single crystals are found in the 1%Ru/CeO_2 sample (see Fig. 5S), which may be from the prolonged room temperature crystallization under condition of high alkali concentration. Here, it can be speculated that a more many and prefect CeO_2 single crystals can be obtained at higher temperature (similar with hydrothermal synthesis method).

3.3. Effect of Ru loading

The catalytic activities and stability of Ru/Ti–CeO_2(5) catalysts (directly marked as Ru/Ti–CeO_2 in later sections) supported different Ru content are investigated and shown in Fig. 6. The catalytic activities increase slightly with the increase of RuO_2 content and reach a maximum at 1.0%, but the difference is negligible especially at lower temperature ranges. However, it can be found that the 0.1% and 0.5%Ru/Ti–CeO_2 catalysts show a lower activity at higher temperature, which can be ascribed to the partial deactivation due to the lower RuO_2 content. The stability tests at 250 °C clearly show the conversion of chlorobenzene over 0.1%Ru/Ti–CeO_2 catalyst dropped from 65% to 20% within 2 h. But, the 0.5%Ru/Ti–CeO_2 catalyst revealed a better stability and was different from the 0.5%Ru/CeO_2 catalyst [28], which probably attributes to the finely dispersion of RuO_2 on Ti–CeO_2 support. Additionally, a small amount of dichlorobenzene by-product was observed only over the 0.5%Ru/Ti–CeO_2 catalyst during stability tests (within 3 h). Eventually, the 1%Ru/Ti–CeO_2 catalyst, the Ti–CeO_2 support containing 5% Ti is prepared by co-precipitation method and tetrabutyl titanate as the precursor, is used for the following further studies.

3.4. Effect of inlet CB concentration and space velocity

The activity of the 1%Ru/Ti–CeO_2 catalyst was evaluated with the catalytic combustion reaction of chlorobenzene under different inlet concentrations and space velocity conditions, and the results are presented in Fig. 7(A) and (B), respectively. As indicated in Fig. 7(A), the conversion of chlorobenzene decreases with the increase of CB concentration. However, the complete

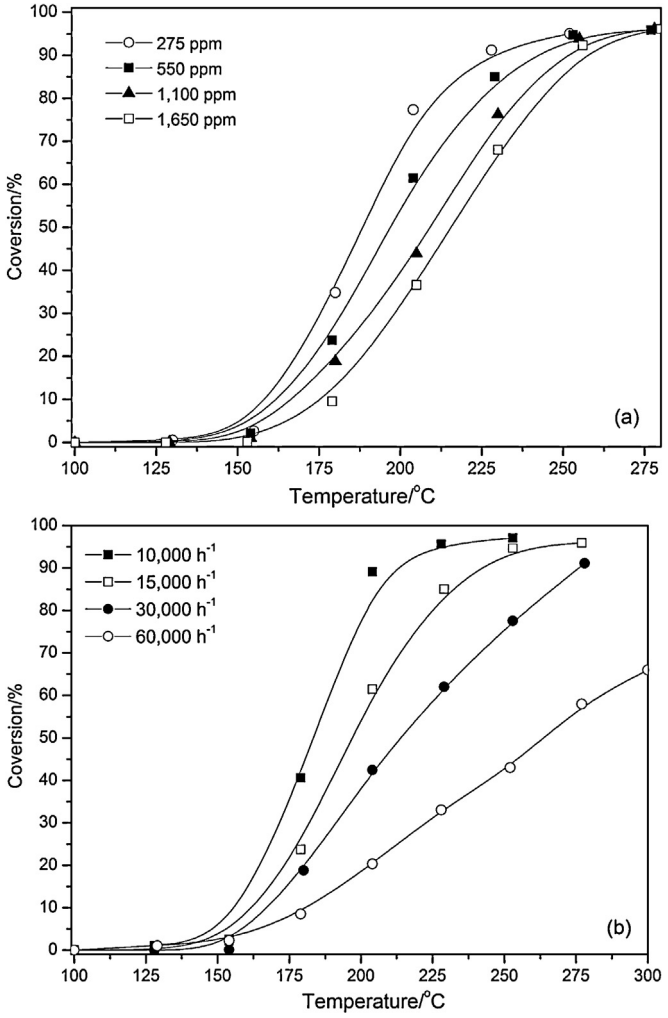

Fig. 7. The light-off curves for CB catalytic combustion under different inlet concentration and space velocity conditions.

conversion can be achieved at 275 °C for the different concentrations of chlorobenzene. This result will be very important to industrial use of the catalysts, because the concentration of pollutants under actual working condition is usually changeable. Additionally, it can be found that the conversion of chlorobenzene decreases with the increase of space velocity because the residence time for feed molecule through catalyst bed decreases with the increase in space velocity, and a suitably high temperature is needed to achieve a sufficient conversion at a higher space velocity, and the only 70% conversion is obtained even at 300 °C under 60,000 h^{-1}.

3.5. Effect of oxygen concentration

Fig. 8 shows the light-off curves of CB catalytic combustion over 1%Ru/Ti–CeO_2 catalyst under different inlet oxygen concentration and the stability at 250 °C. In particular, in order to more directly observe the effect of oxygen, the GHSV is extended to 30,000 h^{-1}. Overall, the activities increase with the increasing of gaseous oxygen concentration, thus, the activation or transform into chemisorbed oxygen species of gaseous oxygen at higher space velocity conditions is an important process for the CB catalytic combustion. Under without gaseous oxygen condition, the activity of 1%Ru/Ti–CeO_2 catalyst is ascribed to the migration of lattice oxygen species into surface oxygen species, and the poor oxidizing ability

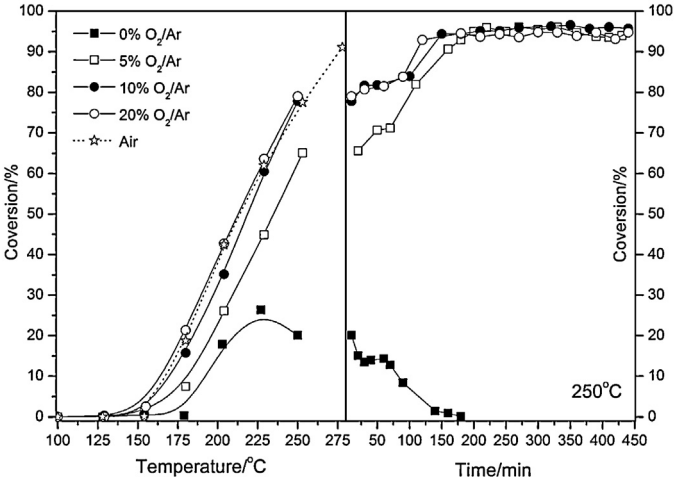

Fig. 8. The light-off curves of CB catalytic combustion over 1%Ru/Ti–CeO_2 catalyst under different inlet oxygen concentrations. CB concentration: 550 ppm; GHSV: 30,000 h^{-1}; catalyst amount: 100 mg; balance Ar.

of lattice oxygen and slower migration result in the lower activity. Additionally, the complete deactivation can be observed after 150 min at 250 °C due to the complete consumption of lattice oxygen species and the adsorption of inorganic Cl species. However, the stability tests indicate that the effect of oxygen concentration on the stable activity is negligible, which probably stems from the good oxygen storage capacity of CeO_2 based materials.

Generally, the oxygen concentration has a more complicated effect on chlorobenzene conversion and byproduct formation [39], thus, the byproduct formation and stability at lower oxygen concentration, GHSV, and higher CB concentration (2.5% oxygen, 15,000 h^{-1} and 1500 ppm) were investigated and the results are shown in Fig. 8S. At 2.5% oxygen, the conversion of CB decreases from 75% to 50% within 3 h and finally is stable (at least 10 h), which is different with the above results from the activity tests. It may be inferred that the higher concentration of CB (1500 ppm) during stability test cannot be completely oxidized due to the lack of adequate oxygen. Additionally, it can be found that the selectivity of the byproduct 1,4-dichlorobenzene is higher at 2.5% oxygen condition compared with at air condition, but the selectivity of 1,2-dichlorobenzene is almost same. We consider that the formation of dichlorobenzene byproducts over Ru based catalysts can be ascribed to the potential chlorination of surface RuO_2 to RuO_xCl_y species [28], and the chlorination is easier and severe at lower oxygen concentration (such as 2.5% oxygen), which is responsible for the high concentration of the polychlorinated byproducts formation.

3.6. Effect of water

The effect of water in the feed on the conversion of CB was investigated and the results are shown in Fig. 9. With addition of 3% water (by volume of reactant gas) into the air containing CB, the activity of CB over the Ti–CeO_2 catalyst without supporting RuO_2 is significantly reduced, and the conversion at 210 °C dropped from 78% to 10%. This inhibition by water probably reflects the competition of the reactant molecules with water molecules for adsorption on the active sites, and the MS results (see Fig. 9S) showed that the CB desorption was not observed under humid condition. However, the 1%Ru/Ti–CeO_2 catalyst shows a better activity below 200 °C under humid condition than under dry condition, which is different with the pervious results of 1%Ru–CeO_2 catalyst [28]. van den Brink et al. also found that the conversion of chlorobenzene over Pt based catalysts was improved in the presence of water [39]. Additionally,

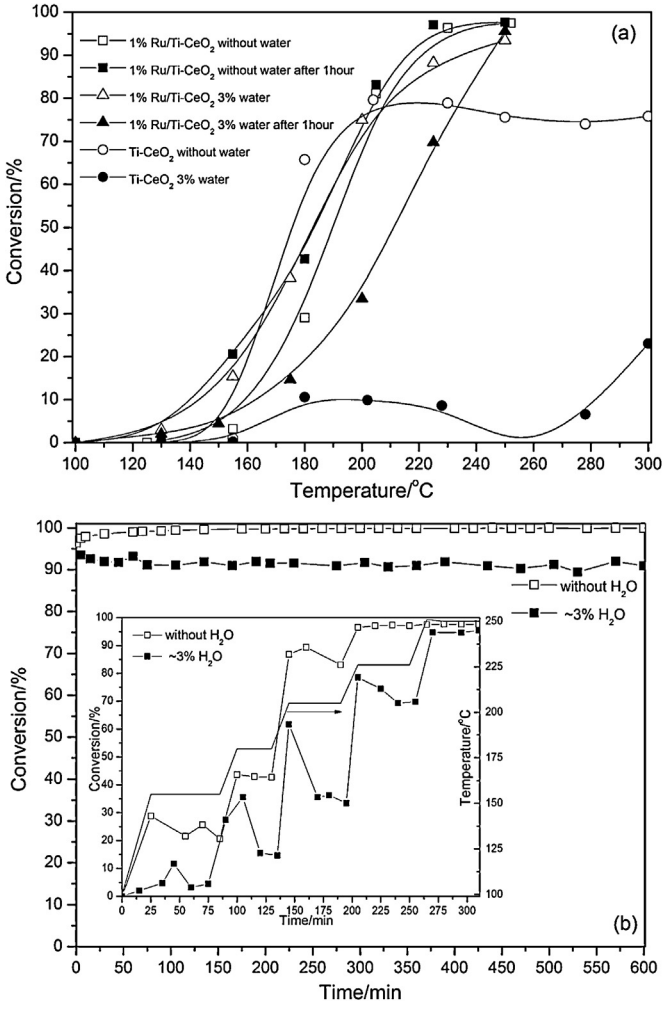

Fig. 9. Conversion and stability of chlorobenzene over Ti–CeO_2 and 1%Ru/Ti–CeO_2 catalysts under dry and water (~3%, v/v) air conditions. CB concentration: 550 ppm; GHSV: 15,000 h^{-1}; catalyst amount: 200 mg.

the stable activity after 1 h reaction at each test temperature under humid and dry conditions also was studied and the results were presented in Fig. 9(A) and (B, inset). Under dry conditions, the stable activity of 1%Ru/Ti–CeO_2 catalyst is higher than the initial activity, which is consistent with the observed phenomenon that there exists an induction period to obtain the highest activity over Ru based catalysts [28]. The deactivation is observed under humid condition (see Fig. 9(B, inset)), and the stable activity is far lower than the initial activity. As yet it is not clear to us which factors determine the variations. Moreover, the stability tests at 250 °C in long time indicate that the 1%Ru/Ti–CeO_2 catalyst demonstrates a good stability whether under dry condition or humid condition, and the formation of higher chlorinated $PhCl_x$ (such as 1,4-dichlorobenzene and 1,2-dichlorobenzene) was suppressed under humid condition. This could be explained by the removal of more Cl in form of HCl from the catalysts surface in the present of water.

3.7. Stability tests

As well known, the stability of catalysts for the catalytic combustion of chlorinated hydrocarbons is a key and trickiest problem, and the deactivation would be observed on the most catalysts due to chlorine poisoning or leaching of active component. Our previous works [28,38] suggested that the introduction of Ru improve evidently the stability of CeO_2 catalysts for the catalytic combustion

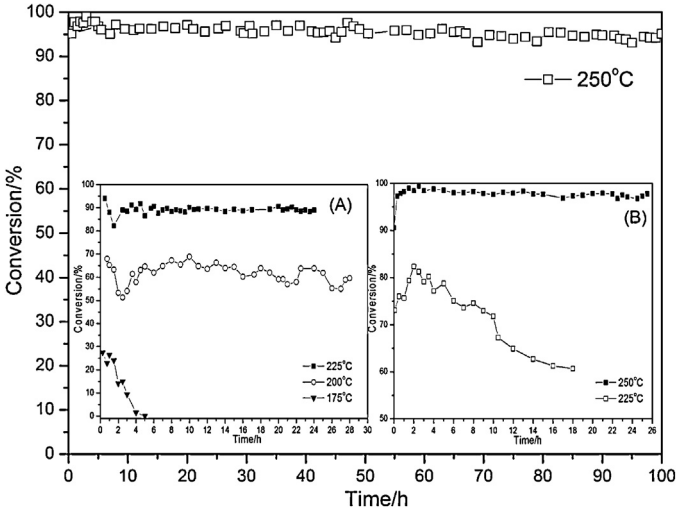

Fig. 10. The stability of 1%Ru/Ti–CeO_2 and 1%Ru/CeO_2 catalysts at different temperatures. (A) 1%Ru/Ti–CeO_2, (B) 1%Ru/CeO_2. CB concentration: 1500 ppm; GHSV: 15,000 h^{-1}; catalyst amount: 200 mg.

of chlorobenzene, however, the desired temperature achieving the better stability still is much higher than the complete combustion temperature and the obvious deactivation can be found at lower temperature. Therefore, the stability tests of 1%Ru/Ti–CeO_2 catalyst at different temperature were carried out and the results are shown in Fig. 10. It can be found that the conversion of chlorobenzene over 1%Ru/Ti–CeO_2 catalyst still can maintain at 95% even after 100 h reaction at 250 °C, by contrast, 1%Ru–CeO_2 catalyst showed an obvious deactivation [28]. The results suggest that the doping of Ti into CeO_2 is favor to improve the stability of 1%Ru–CeO_2 catalyst, which may be ascribed to the good activity of Ru/TiO_2 for the oxidation of HCl (or dissociatively adsorbed Cl species) into Cl_2 [30,31]. However, Fig. 10(inset, B) showed a better stability also can be observed over 1%Ru/CeO_2 catalyst at 250 °C and the 95% conversion is not changed within 26 h. Therefore, the role of Ti improving stability of catalysts cannot be confirmed, and the effect of the method introducing Ru into CeO_2 is not ignored. Comparing with Ru–CeO_2 catalyst prepared by the co-precipitation method, the Ru species in the Ru/CeO_2 or Ru/Ti–CeO_2 catalyst prepared by the impregnation method more finely disperse the surface of supports, which results in the high catalytic activity for the oxidation of HCl and increasing the stability of CeO_2 based catalysts. Subsequently, the stability tests at lower temperature indicated that the deactivation of 1%Ru/CeO_2 catalyst at 225 °C occurs and the conversion drops from 83% to 60% within 18 h, but 1%Ru/Ti–CeO_2 catalyst presents a better stability at 225 °C, even at 200 °C, and the deactivation is only observed until 175 °C (see Fig. 10(inset, A)). Additionally, it can be found that the conversion of chlorobenzene over 1%Ru/Ti–CeO_2 catalyst firstly decreases with reaction time and then increases, eventually stable during stability tests at lower temperatures (especially at 225 °C and 200 °C), which probably results from the re-dispersion of Ru species on the supports (especially on TiO_2) and favors to the removal of the dissociatively adsorbed Cl species from surface of CeO_2.

To further investigate the changes of CB and products (CO_2, HCl and Cl_2) during CB catalytic combustion over Ti–CeO_2, 1%Ru/Ti–CeO_2 and 1%Ru/CeO_2 catalysts, the TPSR technique was used and the results were showed in Fig. 11. According to the real-time monitoring results of CO_2 and CB, it can be found clearly the desorption of CB during raising temperature and the formation of the complete oxidation product (CO_2), moreover, the

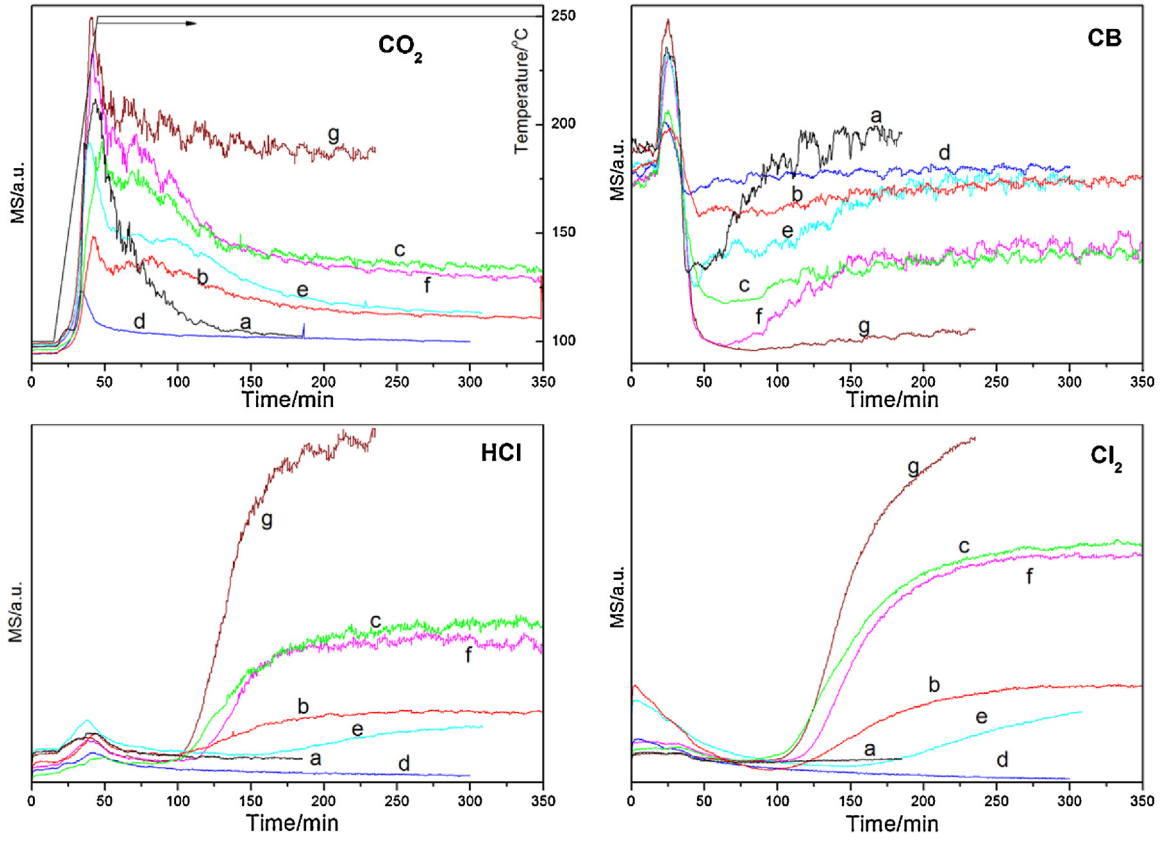

Fig. 11. TPSR profiles for CB catalytic combustion over CeO_2 based catalysts. CB concentration: 1500 ppm; GHSV: 15,000 h^{-1}; catalyst amount: 200 mg.

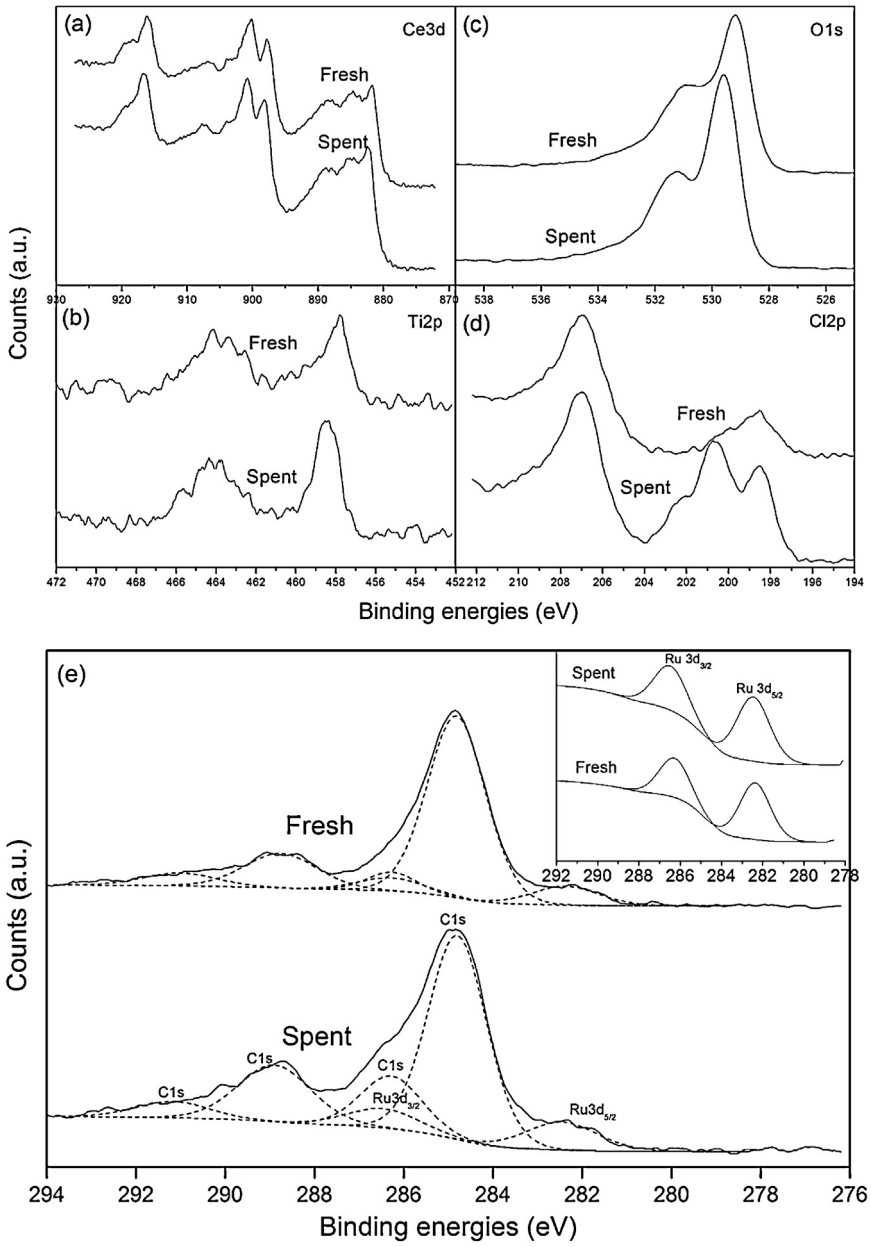

Fig. 12. XPS spectra of the spent and the fresh 1%Ru/Ti–CeO_2 catalysts.

deactivation also can be observed over 1%Ru/Ti–CeO_2 and 1%Ru/CeO_2 catalysts at lower temperature or over Ti–CeO_2 catalyst. These results coincide with stability tests. Additionally, the monitoring of HCl and Cl_2 evolutions showed that its evolutions are difficult and can be monitored only after 90 min, which attributes to the strong adsorption on the catalysts surface (the XPS results confirmed the adsorption of Cl species). Even, the evolutions of HCl and Cl_2 until the complete deactivation of catalysts (such as Ti–CeO_2 at 250 °C and 1%Ru/Ti–CeO_2 at 175 °C) are not observed, which probable is the major reason for the deactivation of catalysts. Meanwhile, it can be found that the amount of HCl and Cl_2 evolutions from 1%Ru/Ti–CeO_2 at 250 °C is much more than that from 1%Ru/CeO_2 at 250 °C, which probably means that the 1%Ru/Ti–CeO_2 catalyst would have a better stability for the catalytic combustion of chlorobenzene or other chlorinated hydrocarbons.

After the reaction, the spent (after 100 h reaction at 250 °C) and the fresh catalysts are characterized by XPS and H_2-TPR. As shown in Fig. 12, after enduring the catalytic test, the changes of Ce 3d XPS spectra are negligible, which shows that the CeO_2 is stable and not chlorinated. Cl 2p emission at 198.6 eV is found in the fresh and spent catalysts, which is associated with Cl species from the $RuCl_3$ precursor and adsorption of HCl and Cl_2 from the decomposition of CB. For the spent catalyst, a peak at 200.5 eV is observed and attributes to chlorobenzene strongly adsorbed on the surface of catalyst. Moreover, the bonding energies of Ru, Ti and O of the spent catalyst shift slightly to the higher bonding energies comparing with the fresh catalyst, which probably from the contamination of chlorobenzene or inorganic chloride species strongly adsorbed on the surface of catalyst. However, the content of the adsorbed oxygen species (the shoulder peak at ca. 531 eV), generally regarded as surface active oxygen species, is not obviously decreased after 100 h reaction at 250 °C and different with the 1%Ru–CeO_2 catalysts [28]. This result suggests that the active sites adsorbing and dissociating the gaseous oxygen can be completely exposed during CB

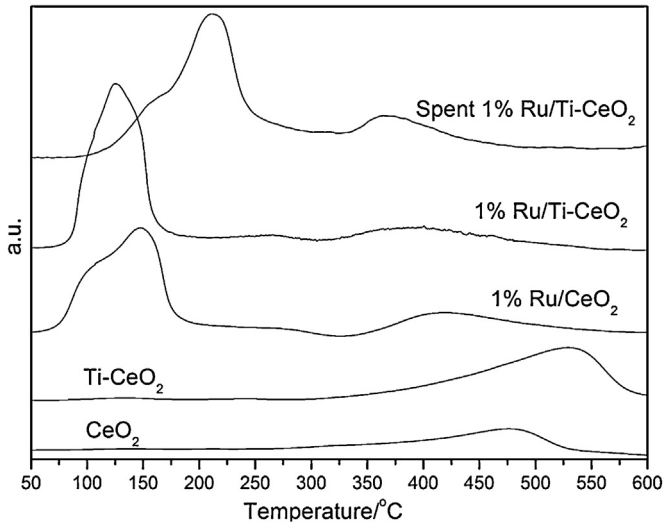

Fig. 13. H_2-TPR of the fresh CeO_2 based catalysts and the spent 1%Ru/Ti–CeO_2 catalyst.

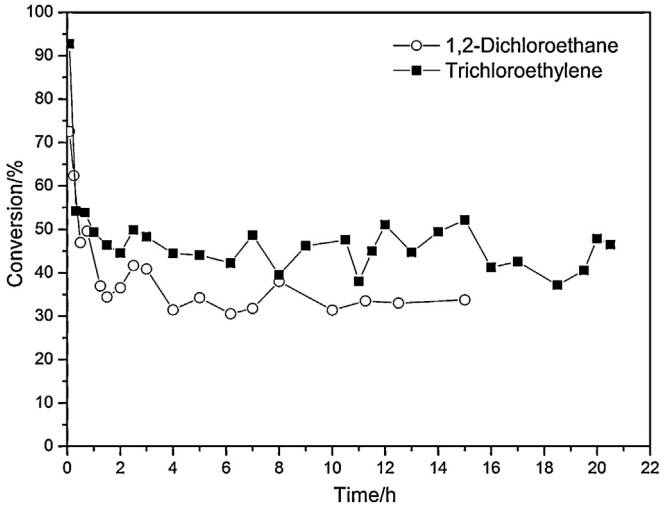

Fig. 14. The stability of 1%Ru/Ti–CeO_2 catalysts at 200 °C for catalytic combustion of 1,2-dichloroethane and trichloroethylene. CHCs concentration: 1500 ppm; GHSV: 15,000 h^{-1}; catalyst amount: 200 mg.

catalytic combustion over 1%Ru/Ti–CeO_2 catalysts, which is favor to the complete oxidation of CB and the better stability of catalysts. Additionally, the ratio of Ru/Ce and Ru/Ti increases from 0.0142 and 0.297 to 0.0155 and 0.360 after the enduring test, respectively, which possibly results from the re-dispersion of Ru species on the Ti–CeO_2 support. The XPS of 1%Ru/Ti–CeO_2 catalyst after different reaction times (such as 1 h and 5 h) at 225 °C also were investigated (see Fig. 10S), and the results are similar with that of after 100 h reaction at 250 °C.

Fig. 13 shows the H_2-TPR of the spent 1%Ru/Ti–CeO_2 catalyst. Comparing with the fresh 1%Ru/Ti–CeO_2, the low temperature peak obviously shifts to the higher temperature, which may be from the strong adsorption of inorganic chloride species on the catalysts surface. Moreover, a new shoulder peak at 175 °C can be found and is similar with the fresh 1%Ru/CeO_2. It can be speculated that the shoulder peak is ascribed to the RuO_2 species highly dispersed on the supports due to the re-dispersion during catalytic combustion reaction, which is consistent with the XPS results. Additionally, the changes of position and area of the peak attributed to the surface active oxygen (between 350 and 450 °C), namely the oxygen species corresponded the shoulder peak at ca. 531 eV in XPS characterization, are almost negligible and also coincides with the XPS results. According to the XPS and H_2-TPR results of the spent 1%Ru/Ti–CeO_2 catalyst, it can be confirmed that the Ru/Ti–CeO_2 catalyst presents a better chemical stability and resistance to the erosion or oxidation of HCl or Cl_2, which is a key factor in improving the stability for CB catalytic combustion.

Additionally, the stability tests of 1%Ru/Ti–CeO_2 catalyst for catalytic combustion of other types of CHCs, such as chlorinated alkanes (e.g. 1,2-dichloroethane, DCE) and chlorinated alkenes (e.g. trichloroethylene, TCE) at low temperature (such as 200 °C) were carried out and the results are shown in Fig. 14, and the activity curves are listed in Fig. 11S. It can be found that 1%Ru/Ti–CeO_2 catalyst also presents a better stability for the catalytic combustion of DCE and TCE, the conversion of DCE and TCE can be maintained at about 35% and 50%, respectively. Moreover, trichloroethane and perchloroethylene as the main by-products of catalytic combustion of DCE and TCE are observed. Combining with the results from CB stability tests, it can be confirmed that the improvement in stability of CeO_2 based catalysts by the loading of Ru and the doping of Ti is general and not related with the type of CHCs.

3.8. Effect of the doping of different metals

Fig. 15 shows the effect of the doping of different metals (such as Sn, Co, Mn and Mg) into CeO_2 on CB catalytic combustion. For the M-CeO_2 without Ru catalysts (see Fig. 15(A)), the CeO_2 doped Ti and Sn catalysts present the highest catalytic activity and the conversion of CB over the Mn doping CeO_2 catalyst is lowest. Additionally, it can be found that the deactivation of the CeO_2 doped Mg, Ti and Sn catalysts is fast, especially Mg–CeO_2 catalyst, which could be attributed to the easy and strong adsorption of inorganic chloride species on the catalyst surface due to the basicity of MgO. Although the doping of Mn and Co more decreases the catalytic activity of CeO_2, the deactivation is not observed during the activity tests, which is consistent with the results reported in literatures [10–14,21]. Generally, transition metal oxides (such as CuO [10,11], MnO_x [12,13], Cr_2O_3 [14] and CoO_x [21]) based catalysts are stable for the catalytic combustion of chlorinated hydrocarbons. However, the deactivation of the Mn and Co doped CeO_2 catalysts still is unavoidable during long-term stability tests, especially at lower temperature. Moreover, the formation of dichlorobenzene by-products over Sn–CeO_2 catalyst are obviously observed, not observed over other metals doped CeO_2 catalysts, which could be ascribed to the formation of Lewis acid due to the fact that SnO_2 can be easily chlorinated into $SnCl_x$ by HCl or Cl_2 during catalytic combustion and Lewis acids ($FeCl_3$, $AlCl_3$, $SbCl_3$, $MnCl_2$, $MoCl_3$, $SnCl_4$ and $TiCl_4$) are used as principal catalysts for the preparation of chlorobenzene or dichlorobenzene in industry [40].

After RuO_2 supported on CeO_2 doped different metals, the decrease of activity over all catalysts during rising temperature is not observed (see Fig. 15(B)), which indicates that the improvement of RuO_2 on the stability of CeO_2 doped different metals is universal and remarkable. Moreover, it was found that the supporting of RuO_2 obviously increases the activities of CeO_2 doped Co and Mn, especially Mn–CeO_2 catalyst. Thus, it can be inferred that the 1%Ru/Mn–CeO_2 catalyst may be a potential and suitable catalyst for the CB catalytic combustion and would be discussed in future works. Additionally, the conversions of other CHCs (such as DCE and TCE) over the 1%Ru/M-CeO_2 catalysts also were investigated, the results suggested that a good activity can be obtained for DCE and TCE, but TCE is more easily oxidized compared with DCE and the complete combustion can be achieved at 200 °C (see Fig. 11S).

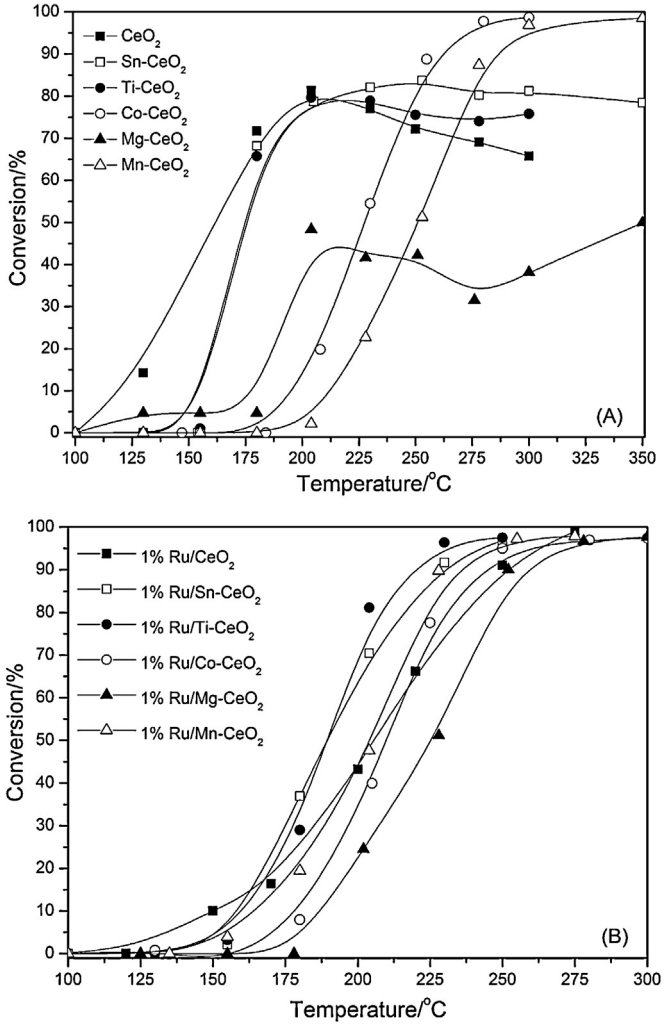

Fig. 15. The conversion of CB over M-CeO_2 and 1%Ru/M-CeO_2 catalysts doped different metals. CB concentration: 550 ppm; GHSV: 15,000 h^{-1}; catalyst amount: 200 mg.

Moreover, Fig. 16 shows the Arrhenius plots of the CB catalytic combustion on 1%Ru/M-CeO_2 catalysts doped different metals according to first order kinetics. It is known that catalytic combustion of VOCs performed in the excess of oxygen can be simplified into a simple reaction pattern described by a first-order kinetic equation [41]. However, a wide range of conditions, not limited to the initial conversions lowering than 10% or 20%, was used at eight different temperatures to obtain a reliable kinetic parameter [42] due to the deactivation of catalysts at lower temperature. According to the slope of the resulting linear plots, the apparent activation energies (E_a) for 1%Ru/CeO_2 and CeO_2 doped Ti, Sn, Mn, Co and Mg are 6.8, 12.2, 7.1, 9.6, 11.4 and 9.5 kJ/mol, respectively. The lower value of activation energy correctly suggested the higher activity of CeO_2 based catalysts compared to the reported catalysts in literatures.

3.9. Effect of the supporting of different precious metals

The supported precious metal catalysts, especially Pt and Pd, are widely used and studied for the catalytic combustion of chlorinated hydrocarbons and have been confirmed to be a kind of catalyst with the highest activity. Therefore, the conversion of chlorobenzene over the 1%PM/Ti–CeO_2 catalysts supported

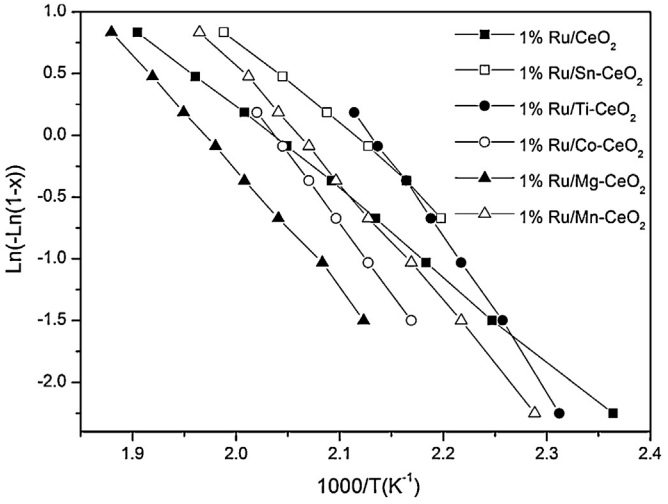

Fig. 16. Arrhenius plots of ln r versus $1/T$ for CB catalytic combustion over 1%Ru/M-CeO_2 catalysts doped different metals.

different precious metals (such as Pt, Pd, Rh, Ru, Au and Ag) and prepared by deposition–precipitation methods was investigated and the results are shown in Fig. 17. The Au and Rh supported Ti–CeO_2 catalysts present a better activity similar with 1%Ru/Ti–CeO_2 catalyst, however, the Pt, Pd and Ag supported Ti–CeO_2 catalysts show a very poor activity (which is very different from the expected activity) and even the obvious deactivation is observed during activity tests. Moreover, it can be found that the supporting method of precious metals except Ru is important and the1%PM/Ti–CeO_2 (PM: Pt, Pd, Rh, Au or Ag) catalysts prepared by incipient wetness impregnation methods give a worse activity (see Fig. 12S). Additionally, the stabilities of Au and Rh supported Ti–CeO_2 catalysts at different temperature and CB concentration (Fig. 13S) and the activities of DCE and TCE over 1%PM/Ti–CeO_2 catalysts (Fig. 14S) also studied. The results indicated that the deactivation of 1%Au or Rh/Ti–CeO_2 catalysts still can be observed at even 275 °C and the other supported precious metals catalysts for the DCE and TCE catalytic combustion also present a lower activity compared with 1%Ru/Ti–CeO_2 catalyst. Summarily, 1%PM/Ti–CeO_2 (PM:Pt, Pd, Rh, Au and Ag) catalyst is not a suitable and promising catalyst for the catalytic combustion of CHCs.

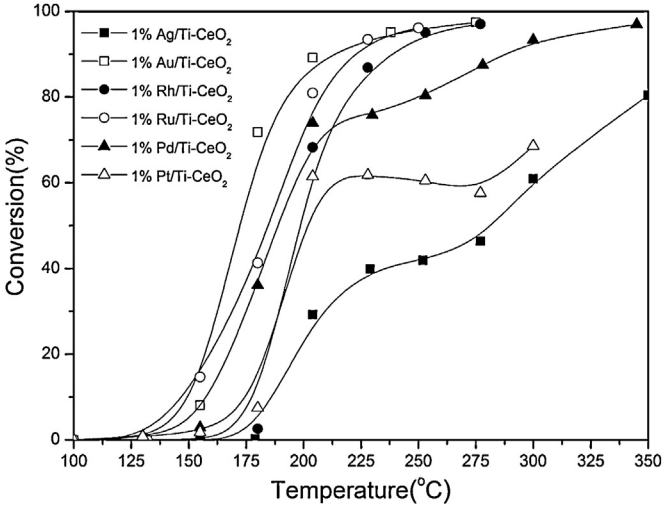

Fig. 17. The conversion of chlorobenzene over the 1%PM/Ti–CeO_2 catalysts supported different precious metals. CB concentration: 550 ppm; GHSV: 15,000 h^{-1}; catalyst amount: 200 mg.

4. Conclusions

The lower temperature catalytic combustion of chlorobenzene over RuO_2 supported on Ti-doped CeO_2 catalysts (Ru/Ti–CeO_2) was investigated, and the effects of preparation methods, Ti content, Ru content, inlet chlorobenzene concentration and space velocity, oxygen concentration and water vapor were studied detailedly. Compared with the Ru/CeO_2 or Ru–CeO_2 catalysts, Ru/Ti–CeO_2 catalyst was found to be a catalyst with better catalytic performance for the chlorobenzene catalytic combustion, and the doping of Ti significantly improved the catalytic activity and stability of CeO_2 based catalysts. The high activity of Ru/Ti–CeO_2 is ascribed to the expose of more oxygen vacancies and high energy lattice plane CeO_2 (1 1 0) and (1 0 0), and the Cl dissociatively adsorbed at active sites of CeO_2 can be oxidized into Cl_2 catalyzed by RuO_2 supported Ti–CeO_2 at lower temperature (such as 200 °C) which be responsible to the excellent stability of Ru/Ti–CeO_2 catalysts.

Moreover, it can be found that Ru/Ti–CeO_2 catalyst also presents a better catalytic activity and stability for the catalytic combustion of other different types of CHCs, such as chlorinated alkanes (e.g. 1,2-dichloroethane) and chlorinated alkenes (e.g. trichloroethylene). In contrast, chlorinated alkanes are harder to be dissociated or oxidized, but the stable conversion can be obtained at low temperature (such as 200 °C) for all of the different CHCs. This result shows that the improvement in stability of CeO_2 based catalysts by the loading or doping of Ru and Ti is general and not related with the type of CHCs, which also indirectly confirms the mechanism proposed in our previous works, namely the deactivation of CeO_2 based catalysts is ascribed to the Cl dissociatively adsorbed at active sites of CeO_2, but this Cl species can be oxidized into Cl_2 catalyzed by RuO_2 and the active sites are re-exposed. The doping of Ti is favor to the oxidation process (namely Deacon process) at lower temperature.

Additionally, the doping of different metals (such as Sn, Co, Mn and Mg) and the supporting of different precious metals (such as Pt, Pd, Ag, Rh and Au) also were explored. The supporting of other precious metals with a lower catalytic activity for the Deacon Reaction does not essentially improve the stability of CeO_2 based catalysts, and the doping of Mn or Co is desired.

In conclusion, the improvement for the stability of CeO_2 based catalysts for the CHCs catalytic combustion by oxidizing the Cl species dissociatively adsorbed at active sites into Cl_2 via Deacon process is feasible, and the employ of RuO_2 with high catalytic activity for Deacon Reaction or TiO_2 with notable promotion effects for RuO_2 catalysts would make CeO_2 based catalysts obtain excellent stability at lower temperature. However, the polychlorinated byproducts still are unavoidable due to the formation of molecular Cl_2, and which becomes a problem need to be solved urgently.

Acknowledgments

This research was supported by Development Program for Young Teachers in Shanghai Universities (No. YJ0153105), National Natural Science Foundation of China (Nos. 20977029, 21277047), Commission of Science and Technology of Shanghai Municipality (No. 11JC1402900) and National Basic Research Program of China (Nos. 2010CB732300, 2011AA03A406).

Appendix A. Supplementary data

Supplementary data associated with this article can be found, in the online version, at http://dx.doi.org/10.1016/j.apcatb.2013.05.026.

References

[1] A. Meharg, Nature 375 (1995) 353–354.
[2] P.H. Taylor, D. Lenoir, Science of the Total Environment 269 (2001) 1–24.
[3] J. Lichtenberger, M.D. Amiridis, Journal of Catalysis 223 (2004) 296–308.
[4] S. Scire, L.F. Liotta, Applied Catalysis B: Environmental 125 (2012) 222–246.
[5] T. Komatsu, R. Ooshima, Journal of the Japan Petroleum Institute 52 (2009) 332–340.
[6] P. Li, C. He, J. Cheng, Z.P. Hao, Acta Physico-Chimica Sinica 25 (2009) 2279–2284.
[7] G. Chiraz, D. Romain, P.D. Damien, E. Pierre, G. Abdelhamid, M.G. Eric, Applied Catalysis A – General 447–448 (2012) 1–6.
[8] Z.Z. Xu, S.B. Deng, Y. Yang, T.T. Zhang, Q.M. Cao, J. Huang, G. Yu, Chemosphere 87 (2012) 1032–1038.
[9] M. Wu, K.C. Ung, Q.G. Dai, X.Y. Wang, Catalysis Communications 18 (2012) 72–75.
[10] X.D. Ma, X. Feng, X. He, H.W. Guo, L. Lv, J. Guo, H.Q. Cao, T. Zhou, Microporous and Mesoporous Materials 158 (2012) 214–218.
[11] X.D. Ma, H.W. Sun, Q. Sun, X. Feng, H.W. Guo, B. Fan, S. Zhao, X. He, L. Lv, Catalysis Communications 12 (2011) 426–430.
[12] Y. Dai, X.Y. Wang, Q.G. Dai, D. Li, Applied Catalysis B: Environmental 111 (2012) 141–149.
[13] H.S. Liang, H.C. Wang, M.B. Chang, Industrial and Engineering Chemistry Research 50 (2011) 13322–13329.
[14] Q.Q. Huang, Z.H. Meng, R.X. Zhou, Applied Catalysis B: Environmental 115–116 (2012) 179–189.
[15] F. Bertinchamps, C. Gregoire, E.M. Gaigneaux, Applied Catalysis B: Environmental 66 (2006) 1–9.
[16] M.A. Larrubia, G. Busca, Applied Catalysis B: Environmental 39 (2002) 343–352.
[17] C. Gannoun, R. Delaigle, P. Eloy, D.P. Debecker, A. Ghorbel, E.M. Gaigneaux, Catalysis Communications 15 (2011) 1–5.
[18] R. Weber, T. Sakurai, H. Hagenmaier, Applied Catalysis B: Environmental 20 (1999) 249–256.
[19] J.M. Giraudon, T.B. Nguyen, G. Leclercq, S. Siffer, J.F. Lamonier, A. Aboukais, A. Vantomme, B.L. Su, Catalysis Today 137 (2008) 379–384.
[20] J.F. Lamoniera, T.B. Nguyena, M. Francoa, S. Siffert, R. Cousin, Y. Lic, X.Y. Yang, B.L. Su, J.M. Giraudona, Catalysis Today 164 (2011) 566–570.
[21] M.H. Kim, K.H. Choo, Catalysis Communications 8 (2007) 462–466.
[22] A. Khalee, A. Al-Nayli, Applied Catalysis B: Environmental 80 (2008) 176–184.
[23] Y. Liu, Z.B. Wei, Z.C. Feng, M.F. Luo, P.L. Ying, C. Li, Journal of Catalysis 202 (2001) 200–204.
[24] W. Tian, X.Y. Fan, H.S. Yang, X.B. Zhang, Journal of Hazardous Materials 177 (2010) 887–891.
[25] M. Kułazynski, J.G. van Ommen, J. Trawczynski, J. Walendziewski, Applied Catalysis B: Environmental 36 (2002) 239–247.
[26] M. Wu, X.Y. Wang, Q.G. Dai, Y.X. Gu, D. Li, Catalysis Today 158 (2010) 336–342.
[27] M. Wu, X.Y. Wang, Q.G. Dai, Y.X. Gu, D. Li, Catalysis Communications 11 (2010) 1022–1025.
[28] Q.G. Dai, S.X. Bai, Z.Y. Wang, X.Y. Wang, G.Z. Lu, Applied Catalysis B: Environmental 126 (2012) 64–75.
[29] Q.G. Dai, S.X. Bai, X.Y. Wang, G.Z. Lu, Applied Catalysis B: Environmental 129 (2013) 580–588.
[30] A.P. Seitsonen, H. Over, Journal of Physical Chemistry C 114 (2010) 22624–22629.
[31] H. Over, Journal of Physical Chemistry C 116 (12) (2012) 6779–6792.
[32] C. Mondelli, A.P. Amrute, F. Krumeich, T. Schmidt, J. Perez-Ramirez, ChemCatChem 3 (2011) 657–660.
[33] D. Teschner, R. Farra, L. Yao, R. Schlogl, H. Soerijanto, R. Schomacker, T. Schmidt, L. Szentmiklosi, A.P. Amrute, C. Mondelli, J. Perez-Ramirez, G. Novell-Leruth, N. Lopez, Journal of Catalysis 285 (2012) 273–284.
[34] J. Perez-Ramirez, C. Mondelli, T. Schmidt, O.F.K. Schluter, A. Wolf, L. Mleczko, T. Dreier, Energy & Environmental Science 4 (2011) 4786–4799.
[35] C.B. Zhang, H. He, K.I. Tanak, Applied Catalysis B: Environmental 65 (2006) 37–43.
[36] M. Triki, Z. Ksibi, A. Ghorbel, F. Medina, Microporous and Mesoporous Materials 117 (2009) 431–435.
[37] P. Panagiotopoulou, J. Papavasiliou, G. Avgouropoulos, T. Ioannides, D.I. Kondarides, Chemical Engineering Journal 134 (2007) 16–22.
[38] Q.G. Dai, H. Huang, Y. Zhu, W. Deng, S.X. Bai, X.Y. Wang, G.Z. Lu, Applied Catalysis B: Environmental 117 (2012) 360–368.
[39] R.W. van den Brink, M. Krzan, R.M.M. Feijen-Jeurissen, R. Louw, P. Mulder, Applied Catalysis B: Environmental 24 (2000) 255–264.
[40] M. Rossberg, W. Lendle, G. Pfleiderer, Ullmann's Encyclopedia of Industrial Chemistry, Wiley-VCH Verlag GmbH & Co. KGaA, 2000.
[41] T.F. Garetto, E. Rincon, C.R. Apesteguia, Applied Catalysis B: Environmental 48 (2004) 167–174.
[42] K.S. Song, D. Klvana, J. Kirchnerova, Applied Catalysis A – General 213 (2001) 113–121.